# Novel Engineered Trastuzumab Conformational Epitopes Demonstrate In Vitro and In Vivo Antitumor Properties against HER-2/*neu*[1]

**Joan T. Garrett,*† Sharad Rawale,* Stephanie D. Allen,*‡ Gary Phillips,§ Guido Forni,# John C. Morris,** and Pravin T. P. Kaumaya[2]*†‡¶‖**

**Trastuzumab is a growth-inhibitory humanized Ab targeting the oncogenic protein HER-2/*neu*. Although trastuzumab is approved for treatment of advanced breast cancer, a number of concerns exist with passive immunotherapy. Treatment is expensive and has a limited duration of action, necessitating repeated administrations of the mAb. Active immunotherapy with conformational B cell epitopes affords the possibility of generating an enduring immune response, eliciting protein-reactive high-affinity anti-peptide Abs. The three-dimensional structure of human HER-2 in complex with trastuzumab reveals that the Ag-binding region of HER-2 spans residues 563–626 that comprises an extensive disulfide-bonding pattern. To delineate the binding region of HER-2, we have designed four synthetic peptides with different levels of conformational flexibility. Chimeric peptides incorporating the measles virus fusion "promiscuous" T cell epitope via a four-residue linker sequence were synthesized, purified, and characterized. All conformational peptides were recognized by trastuzumab and prevented the function of trastuzumab inhibiting tumor cell proliferation, with 563–598 and 597–626 showing greater reactivity. All epitopes were immunogenic in FVB/N mice with Abs against 597–626 and 613–626 recognizing HER-2. The 597–626 epitope was immunogenic in outbred rabbits eliciting Abs which recognized HER-2, competed with trastuzumab for the same epitope, inhibited proliferation of HER-2-expressing breast cancer cells in vitro and caused their Ab-dependent cell-mediated cytotoxicity. Moreover, immunization with the 597–626 epitope significantly reduced tumor burden in transgenic BALB-*neu*T mice. These results suggest the peptide B cell immunogen is appropriate as a vaccine for HER-2-overexpressing cancers because the resulting Abs show analogous biological properties to trastuzumab.** *The Journal of Immunology,* **2007, 178: 7120–7131.**

The tumor Ag HER-2 (ErbB2), a member of the epidermal growth factor receptor family, consists of a cysteine-rich extracellular domain (ECD)[3] that has several glycosylation sites, a transmembrane domain, and an intracellular conserved tyrosine kinase domain (1). Lacking a high-affinity ligand, HER-2 functions as a preferential heterodimerization-signaling partner with other members of the EGFR family (EGFR, HER-3, and HER-4) (2, 3) leading to cellular proliferation and differentiation. HER-2 is weakly detectable in epithelial cells of normal tissues (4), but is frequently overexpressed in cancers of the breast, ovary, uterus, lung, and gastrointestinal tract (5–9). HER-2 overexpression in breast cancer patients is associated with a poor prognosis (10). These findings make HER-2 an ideal target for cancer immunotherapy.

Numerous Abs directed against the ECD of HER-2 have been generated by immunizing mice with cells expressing HER-2. Dependent upon epitope specificity, the interaction of HER-2 and anti-HER-2 Abs resulted in no effect, inhibition, or stimulation of tumor growth (11). Trastuzumab (Herceptin), a humanized mAb directed against HER-2, has been shown to cause phenotypic changes in tumor cells including down-regulation of the HER-2 receptor, inhibition of tumor cell growth, and reduced vascular endothelial growth factor production (12). In addition, the interaction of trastuzumab with the human immune system via its human IgG1 Fc domain may promote its antitumor properties. In vitro and in vivo studies prove that trastuzumab is very effective in mediating Ab-dependent cell-mediated cytotoxicity (ADCC) against HER2-overexpressing tumor cell lines (13). Trastuzumab is FDA approved for passive immunotherapy in patients with metastatic HER-2-overexpressing breast cancer. In addition, recent studies indicate that 12 mo of trastuzumab treatment along with chemotherapy significantly reduced disease recurrence in patients with early stage breast cancer (14, 15). Trastuzumab has recently been approved in combination with doxorubicin, cyclophosphamide, and paclitaxel in adjuvant treatment for early stage breast cancer after primary therapy.

There are a number of concerns despite the impressive clinical effects of passive trastuzumab application, these include limited duration of action that necessitates repeated treatments at considerable cost. Trastuzumab treatment has been linked with side effects including cardiac dysfunction and congestive heart failure (14–17). The induction of humoral immune responses against HER-2 using active immunotherapy generating a polyclonal, long-lasting immune response has become a desirable objective. To this

*Departments of Obstetrics and Gynecology, †Chemistry Biology Interface Program, ‡Ohio State Biochemistry Program, §Center for Biostatistics, ¶Molecular Virology, Immunology, Medical Genetics, and ‖Arthur G. James Comprehensive Cancer Center, Ohio State University, Columbus, OH 43210; #Molecular Biology Center, Department of Clinical and Biological Sciences, University of Turin, Turin, Italy; and **Metabolism Branch, Center for Cancer Research, National Cancer Institute, Bethesda, MD 20892

Received for publication August 9, 2006. Accepted for publication March 12, 2007.

The costs of publication of this article were defrayed in part by the payment of page charges. This article must therefore be hereby marked *advertisement* in accordance with 18 U.S.C. Section 1734 solely to indicate this fact.

[1] This work was supported by National Cancer Institute Grant CA 84356 (to P.T.P.K.).

[2] Address correspondence and reprint requests to Dr. Pravin T. P. Kaumaya, The Ohio State University, Suite 316 Medical Research Facility, 420 West 12th Avenue, Columbus, OH 43210. E-mail address: kaumaya.1@osu.edu

[3] Abbreviations used in this paper: ECD, extracellular domain; ADCC, Ab-dependent cell-mediated cytotoxicity; MVF, measles virus fusion protein; CDC, complement-dependent cytotoxicity; CD, circular dichroism; ESI-MS, electrospray ionization mass spectroscopy; HER-2, human epidermal growth factor receptor; PEO, polyethyleneoxide.

end, our laboratory has studied a number of epitopes from the HER-2 ECD identified from computer-aided analysis; we reported the antitumor properties of chimeric B cell epitope sequences 628–647 and 316–339 that incorporate a promiscuous T cell epitope (measles virus fusion protein (MVF)) (18, 19). These studies are the basis for the phase I clinical trial currently being conducted at The Ohio State University James Cancer Hospital.

The crystal structure of the trastuzumab Fab bound to HER-2 reveals that it binds at the C-terminal portion of subdomain IV of the HER-2 ECD (20) which should facilitate the design of new therapeutics and vaccines. Trastuzumab binds the C-terminal end of domain IV of the extracellular region of HER-2 amino acids 579–625. Binding of trastuzumab blocks activation of HER-2 by promoting receptor endocytosis as well as blocking proteolytic cleavage of the ECD. Thus, the selection, design, and syntheses of selected regions allow us by active immunization to generate sequence-specific anti-peptide Abs. By examining the mechanistic effects of these Abs such as induction of apoptosis, decreased cell proliferation, Her-2 down-regulation, dephosphorylation, inhibition of signal pathways, inhibition of homo/heterodimerization, ADCC, and complement-dependent cytotoxicity (CDC), we are then able to select these readouts as guides for pursuing in vivo studies as well as for translating these vaccines to the clinic.

In particular, Abs raised against a peptide that could closely mimic the native structure of the pocket-like trastuzumab-binding region of HER-2 are likely to provide more effective functional cross-reactive immune responses with potent antitumor properties. We have successfully used several different strategies to mimic the conformation of epitopes in native proteins (21–24). We also demonstrated the use of peptide cyclization by incorporating native disulfide bonds in the 626–649 sequence of HER-2/neu (24) which resulted in improved in vitro and in vivo activity compared with the linear noncyclized peptide.

In this study, we have designed several HER-2 epitopes at the HER-2/trastuzumab interface requiring an elaborate scheme for the successful synthesis, purification, and characterization of these complex epitopes. We show that with varying degrees of reactivity all conformationally restricted peptides were recognized by trastuzumab and blocked the function of trastuzumab inhibiting tumor cell proliferation. All the cyclic and linear epitopes were highly immunogenic in inbred mice eliciting high titered Abs. The 597–626 and 613–626 epitopes elicited strong native-like anti-peptide Abs as evidenced by their reactivity to BT474 and SK-BR-3 breast cancer cell lines using flow cytometric analysis. The 597–626 epitope was immunogenic in outbred rabbits eliciting Abs that recognized HER-2 at the HER-2/trastuzumab interface, inhibited cancer cell growth in vitro, and caused Ab-dependent cell-mediated cytotoxicity. To investigate the efficacy of vaccination in a clinically relevant model, we examined the ability of the conformationally restricted 597–626 epitope as well as its linear counterpart to inhibit the development of mammary tumorigenesis in a transgenic model of HER-2/*neu* in which the HER-2/neu oncogene is expressed in a tissue-specific manner. We demonstrated that immunization with the 597–626 epitope significantly reduced tumor burden in this aggressive tumor model. We conclude the HER-2 597–626 sequence is a potential vaccine candidate that could be translated to the clinic.

## Materials and Methods

### *Synthesis of linear and disulfide-constrained peptides*

HER-2 B cell epitopes 563–598, 585–598, 597–626, and 613–626 were synthesized colinearly with a promiscuous Th epitope derived from the measles virus fusion protein (amino acid 288–302). Peptide synthesis was performed on a Milligen/Biosearch 9600 peptide solid-phase synthesizer using F-moc/t-But chemistry on preloaded clear acid resin (Peptides International) and cleaved using reagent B (trifluoroacetic acid:phenol:water: triisopropylsilane, 90:4:4:2). Three disulfide bonds were introduced in the epitope HER-2 563–598 to more closely mimic the three-dimensional structure of HER-2 protein. Chemoselective protecting groups Cys(Trt), Cys(Acm), Cys(But) were used for desired disulfide paring. The protecting group from Cys(Trt) comes off in the global cleavage reaction as confirmed by electrospray ionization mass spectroscopy (ESI-MS) analysis. Pure fractions were analyzed using analytical Waters HPLC, pooled together, and lyophilized in 1% acetic acid solution. Cleavage of the peptide, reverse-phase-HPLC purification, and lyophilization in acidic medium and prevention of oxidation of free sulfhydryl groups of Cys residues as confirmed by ESI-MS analysis was performed.

### *Circular dichroism (CD) measurements*

Aqueous solutions for CD were prepared by dissolving the freeze-dried peptide in the appropriate amount of water to give a final concentration of 0.5 mM and were used as stock solution for further dilution. CD spectra were recorded on an AVIV model 62A DS CD instrument as reported earlier (24). Mean residue ellipticity ($(\theta)_{M,\lambda}$) values were calculated according to the equation: $(\theta)_{M,\lambda} = (\theta \times 100 \times M_r)/(n \times c \times l)$. Where $\theta$ is the recorded ellipticity (deg), $M_r$ the m.w. of the peptide, $n$, the number of residues in the peptide, $c$, the peptide concentration (milligrams per milliliter), and $l$, the path length of the cuvette. Helicity of peptides was determined according to Chen et al. (25) with reference to mean residue ellipticity of polylysine for 100% $\alpha$-helix $(\theta)_{222} = -35{,}700$ (26).

### *Animals*

Female New Zealand White outbred rabbits and FVB/n inbred mice were purchased from Harlan Breeders. Virgin female BALB-neuT mice (27), BALB/c mice transgenic for the rat-transforming *neu* oncogene expressed under the control of mouse mammary tumor virus promoter, were bred in our animal facility. Animal care and use was in accordance with institutional guidelines.

### *Cell lines and Abs*

All cell culture medium, FCS, and supplements were purchased from Invitrogen Life Technologies. The human breast tumor cell lines, BT-474, SK-BR-3, and MDA-468, were purchased from American Type Culture Collection and maintained according to the supplier's guidelines. TUBO cells are a cloned cell line established in vitro from a lobular carcinoma that arose spontaneously in a BALB-*neu*T mouse (28). TS/A cells are derived from a spontaneous breast cancer of a wild-type BALB/c mouse. HER-2 mAb Ab-2 (clone 9G6) was purchased from Neomarkers. Rat neu mAb Ab-4 was purchased from Calbiochem. Humanized mouse mAb Herceptin (trastuzumab) was provided by Genentech (South San Francisco, CA).

### *Immunoassays*

To determine the ability of trastuzumab to bind various peptides, a trastuzumab-specificity ELISA was performed. Ninety-six-well plates were coated with 100 $\mu$l of peptide at 2 $\mu$g/ml in PBS overnight at 4°C. Nonspecific binding sites were blocked for 1 h with 200 $\mu$l of PBS-1% BSA, and plates were washed with phosphate-buffered Tween 20. Trastuzumab (2 mg/ml) was added to Ag-coated plates in duplicate wells, serially diluted 1:2 in PBT, and incubated for 2 h at room temperature. After washing the plates, 100 $\mu$l of 1:500 goat anti-human IgG conjugated to HRP (Pierce) were added to each well and incubated for 1 h. After washing, the bound Ab was detected using 50 $\mu$l of 0.15% $H_2O_2$ in 24 mM citric acid and 5 mM sodium phosphate buffer (pH 5.2) with 0.5 mg/ml ABTS as the chromophore. Color development was allowed to proceed for 10 min and the reaction was stopped with 25 $\mu$l of 1% SDS. Absorbance was determined at 410 nm using a Benchmark Microplate Reader (Bio-Rad).

Determining the antipeptide response was performed as previously described (18). Ab titers were defined as the reciprocal of the highest serum dilution with an absorbance of 0.2 or greater after subtracting the background. All data represent the average of duplicate samples.

Mouse serum was isotyped using Mouse Typer SubIsotyping kit (Bio-Rad) which was used per the manufacturer's instructions. Rabbit serum was isotyped using goat anti-rabbit IgG, IgM, and IgA conjugated to HRP (Novus Biologicals).

To determine the anti-HER-2 response, a sandwich ELISA was performed. Plates were coated overnight at 4°C with 100 $\mu$l of 10 $\mu$g/ml Ab-2, washed four times with 0.1% Tween 20/PBS, and blocked with 100 $\mu$l of PBS-1% BSA for 4 h on a rocker. Plates were washed four times with 0.1% Tween 20/PBS. Wells were then coated overnight at 4°C with 50 $\mu$l of either PBS-1% BSA or SK-BR-3 cell lysate ($1 \times 10^8$ cells in 20 ml of lysis

buffer). Lysis buffer was composed of 1% Triton X-100, 10% glycerol, 150 mM NaCl, 50 mM HEPES, 1.5 mM $MgCl_2$, 1 mM EDTA, 10 mM pyrophosphate, 100 mM NaF, 0.2 mM $Na_3VO_4$, 10 $\mu$g/ml aprotinin, 10 $\mu$g/ml leupeptin, and 1 mM PMSF. Plates were washed four times with 0.1% Tween/PBS and serial dilutions of rabbit sera (starting at 1/100) were added and the plates were incubated for 2 h on a rocker. Ab binding was detected as described above.

The anti-HER-2 response was measured using a second competitive inhibition assay: plates were coated overnight at 4°C with 100 $\mu$l of 500 ng/ml recombinant human HER-2 ECD/Fc chimera (R&D Systems) and plates blocked with 2%BSA for 1 h at 25°C. A constant amount (1/2000 dilution) of rabbit anti-597–626 CYC abs or anti-597–626 NC abs was added to the plates and at the same time various amounts of inhibitor (trastuzumab or isotype control human IgG) was added. Bound anti-peptide rabbit Abs was detected with HRP-conjugated anti-rabbit IgG Ab (minimized for binding human IgG). The inhibition rate was calculated according to the following formula: $(OD_{\text{anti-peptide Ab}} - OD_{\text{anti-peptide Ab + inhibitor}})/(OD_{\text{anti-peptide Ab}}) \times 100$.

### *Peptide immunization and Ab purification*

Mice and rabbits were immunized s.c. at multiple sites with a total of 1 mg (rabbits) or 100 $\mu$g (mice) of peptide dissolved in $H_2O$ with 100 $\mu$g of a muramyl dipeptide adjuvant, nor *N*-acetyl-glucosamine-3 yl-acetyl L-alanyl-D-isoglutamine (MDP). Peptides were emulsified (50:50) in Seppic Montanide ISA 720 vehicle. The same dose of booster injections was administered twice at 3 and 6 wk. Sera were collected and complement was inactivated by heating to 56°C for 30 min. High-titered sera were purified on a protein A/G agarose column (Pierce) and eluted Abs were concentrated and exchanged in PBS using 100-kDa cutoff centrifuge filter units (Millipore). The concentration of Abs was determined by Coomassie plus protein assay reagent (Pierce).

BALB-*neu*T mice were immunized in the same manner described, commencing at 5–6 wk of age. After the second boost, the transgenic mice received two subsequent boosters at monthly intervals. Tumor size (length and width) in each of 10 mammary glands was measured twice weekly with Vernier calipers beginning at 18 wk of age. Individual tumors were calculated by the formula (length $\times$ width$^2$)/2. All mice were euthanized at 25 wk of age.

### *Flow cytometry*

A total of $1 \times 10^6$ BT474, SK-BR-3, TUBO, or MDA468 cells were incubated with 1, 10, or 100 $\mu$g of mouse or rabbit antipeptide Abs. HER-2-specific mouse mAb Ab-2 (Lab Vision) and rat neu-specific mAb Ab-4 (Calbiochem) were used as positive controls, and isotypic IgG was used as a negative control. Cells were incubated for 2 h at 4°C in 100 $\mu$l of PBS/2% FCS/0.1% $NaN_3$. The cells were washed twice in cold PBS and incubated with FITC-labeled secondary Ab (1/50 dilution) for 30 min at 4°C in 100 $\mu$l of PBS/1% FCS/0.1% $NaN_3$. The cells were washed twice, fixed in 1% formaldehyde, and analyzed by a FACSCalibur flow cytometer (BD Biosciences). A total of 10,000 cells were counted for each sample and final processing was performed. Debris, cell clusters, and dead cells were gated out by light-scattered assessment before single-parameter histograms were drawn and smoothed.

### *Cell survival assay by trypan blue exclusion*

This assay was adapted from Nahta et al. (29). BT474 cells were seeded at a density of $1 \times 10^5$ cells/well in 12-well plates. Twenty-four hours later, cells were treated in triplicate with 20 $\mu$g/ml anti-peptide Abs, trastuzumab, or normal rabbit IgG for an additional 72 h. Cells were trypsinized and stained with trypan blue dye and viable cells were counted under a microscope. Cell growth inhibition is expressed as the percentage of viable cells compared with untreated cells.

### *MTT cell growth inhibition assay*

For peptides preventing trastuzumab from inhibiting tumor cell growth assay, BT474 cells were plated in 96-well microtiter plates at $2 \times 10^4$ cells/well and incubated overnight at 37°C. PBS-containing trastuzumab or normal human IgG (100 $\mu$g/ml) with or without dilutions of peptide was added to the wells. The plates were incubated for 3 days at 37°C. The number of viable cells was measured with MTT by reading $OD_{570}$. The percentage of inhibition was calculated using the formula $(OD_{\text{normal human IgG}} - OD_{\text{trastuzumab + peptide}})/OD_{\text{normal human IgG}} \times 100$. All experiments were performed in triplicate.

For anti-peptide Abs inhibiting tumor cell growth, the assay was performed in a similar fashion with several modifications. BT474 cells were plated at $1 \times 10^4$ cells/well and the following day were treated with 0.1 $\mu$g/ml rabbit anti-peptide Abs, trastuzumab, or normal rabbit IgG in triplicate for an additional 72 h. The percentage of inhibition was calculated using the formula $(OD_{\text{normal rabbit IgG}} - OD_{\text{peptide Ab}})/OD_{\text{normal rabbit IgG}} \times 100$.

### *ADCC*

Effector PBMCs from normal human donors obtained by density gradient centrifugation in Ficoll-Hypaque (Pharmacia Biotech) were washed twice in RPMI 1640–5% FCS and then serially diluted in 96-well plates to give E:T ratios of 25:1, 12.5:1, and 6.25:1. The following day, $1 \times 10^6$ target cells received 50 $\mu$g of protein A/G-purified anti-peptide rabbit Abs or trastuzumab (Genentech). BT-474 and MDA-468 target cells (HER-2$^{high}$ and HER-2$^{low}$, respectively) were labeled with 100 $\mu$Ci/$1 \times 10^6$ cells of $Na^{51}CrO_4$ (PerkinElmer) and incubated for 1 h at 37°C. After three washings, $5 \times 10^3$ target cells were delivered to each well so as to give a final volume of 0.2 ml/well. The cells were incubated for 4 h at 37°C, after which time 75 $\mu$l of cell-free supernatants were harvested and radioactivity determined using a gamma counter. To assess nonspecific lysis effector and target cells were coincubated in the presence of normal rabbit Abs. Cytotoxicity was calculated by the formula (percent) lysis = $(A - B)/(C - B) \times 100$, where $A$ represents $^{51}$Cr (cpm) from test supernatants, $B$ represents $^{51}$Cr (cpm) from target alone in culture (spontaneous release), and $C$ represents maximum $^{51}$Cr release from target cells lysed with 5% Triton X-100. Results represent the average of triplicate samples.

### *Statistical analysis*

Differences in MTT cell proliferation assay were evaluated with the Student $t$ test. Tumor growth over time was analyzed using Stata's XTGEE (cross-sectional generalized estimating equations) model which fits general linear models that allow you to specify within animal correlation structure in data involving repeated measures. The model includes terms for treatment group, time, and the interaction of treatment by time. This interaction term is used to calculate the differences in the slopes of each group. The XTGEE model assumes that the data are normally distributed and that volume is a continuous linear variable. Log transformation of the volume addresses both of these issues. The slopes by treatment of the log-transformed tumor volumes were calculated and compared with determine whether there was a statistically significant difference between treatments. The significance level was set at $\alpha = 0.01$ to control for the overall type I error rate when doing multiple comparisons. The results of the above regression are transformed back into their original units.

## Results

### *Design and synthesis of conformational and linear peptides*

The crystal structure of the extracellular region of HER-2 bound to the trastuzumab Fab reveals that trastuzumab binds subdomain IV of the HER-2 ECD (20). The Ag-Ab interaction is mediated by three regions of HER-2. These regions are composed of loops which consist of residues 579–583 (formed by two disulfide bonds; C563-C576 and C567-C584), 592–595 (cysteine disulfide pairing between C587-C596), and 615–625 (cysteine disulfide bond between C600-C623). We have selected this 64 residue cysteine-rich region of the HER-2 ECD for the design of several peptides to minimally mimic the binding epitope. Four constructs (Table I) encompassing residues 563–626 were designed to contain as least one region of the three binding sequences that make contact with trastuzumab. In addition, we have incorporated the native disulfide bonds in each of these epitopes.

Epitopes containing one or two intramolecular disulfide bond were cyclized using iodine oxidation and characterized as reported (24). In the case of epitope MVF 563–598, which contains three intramolecular disulfide bonds, the first and second disulfide bond formation was performed with in situ reaction using $I_2/H_2O$, the first disulfide bond formation occurring in the first hour. The addition of water boosts the removal of acetamidomethyl groups and concurrent formation of second disulfide bond. This was confirmed by polyethyleneoxide (PEO)-maleimide reaction; biotinylation agent PEO-maleimide, which attacks free sulfhydryl groups to form addition product and therefore can be used to determine the completion of disulfide pairing and was confirmed by ESI-MS (24). Two Cys(Bu$^t$) groups remained intact during the cyclization

Table I. *Peptides synthesized from the trastuzumab-binding region of HER-2*

| Designation[a] | Peptide | Sequence[b] |
|---|---|---|
| 563 CYC | 563–598<br>Three disulfide bonds | CHPECQPQNGSVTCFG**PEADQ**CVACAHYK**DPPF**CVA |
| 585 CYC | 585–598<br>One disulfide bond | VACAHYK**DPPF**CVA |
| 597 CYC | 597–626<br>One disulfide bond | VARCPSGVKPDLSYMPIW**KFPDEEGACQP**L |
| 613 | 613–626 | IW**KFPDEEGACQP**L |

[a] Peptides containing disulfide bonds (CYC) are shown; linear versions (NC) were also synthesized (not shown in table).
[b] Residues involved in binding trastuzumab are shown in bold; a possible *N*-linked glycosylation site in the 563–598 epitope is boxed. Underlined amino acids were mutated from Cys to Leu so as not to interfere with natural disulfide formation.

procedure. The third disulfide bond was formed by silyl-chloride-sulfoxide method and the completion of third disulfide bond was confirmed by PEO-maleimide reaction; no PEO-maleimide addition was observed, which was confirmed by ESI-MS characterization (Fig. 1). Linear peptide was generated by DTT reduction. These spectroscopic results indicate that we have successfully synthesized conformational peptides incorporating three disulfide bonds.

The HER-2 B cell epitopes were synthesized colinearly with a promiscuous Th epitope derived from the measles virus fusion protein (MVF) (amino acids 288–302). A four-residue linker sequence, GPSL, connects the Th and B cell epitopes; this linker sequence forms a hairpin loop. The small, flexible nature of glycine and the ability of proline to readily form the *cis*-conformer make these amino acids amenable to tight turns. Serine favors hydrogen bonds with the free amide of the backbone and interacts favorably with solvent and leucine is buried in the hydrophobic core. Independent folding of the Th and B cell epitopes is achieved using the flexible linker sequence (30, 31).

### *Specificity of peptides binding to trastuzumab*

To examine the ability of trastuzumab to bind the conformational cyclized synthetic peptides, a trastuzumab specificity ELISA was developed. Polystyrene plates were coated overnight with various peptides and the following day probed with trastuzumab. Trastuzumab binds to all four of the peptides MVF 563–598, 585–598, 597–626, and 613–626 but not the irrelevant control peptide MVF 316–339 (Fig. 2*A*). The 563–598 peptide exhibited the highest reactivity with the mAb. Moreover, trastuzumab binds the synthetic peptide MVF 563–598 that incorporates the natural disulfide pairings of HER-2 in a dose-dependent manner and to a lesser extent the linear noncyclized peptide (Fig. 2*B*). These results suggest that the conformation induced by cyclization mimics the native sequence better than the flexible peptide.

### *Conformational peptides prevent trastuzumab inhibiting tumor cell growth*

The ability of trastuzumab to bind the ECD of HER-2 and inhibit the downstream signaling of HER-2, resulting in growth inhibition of HER-2-overexpressing cell lines has been demonstrated extensively (13). Because we have shown that trastuzumab recognizes all four of the peptides, we investigated whether theses peptide prevent trastuzumab from inhibiting tumor cell growth. By preincubating trastuzumab with peptide, the response rate of the breast cancer cell line BT474 to trastuzumab was blocked by all peptides (MVF 563–598CYC, MVF 585–598CYC, MVF 597–626CYC, and MVF 613–626) in a dose-dependent manner, while an equivalent concentration

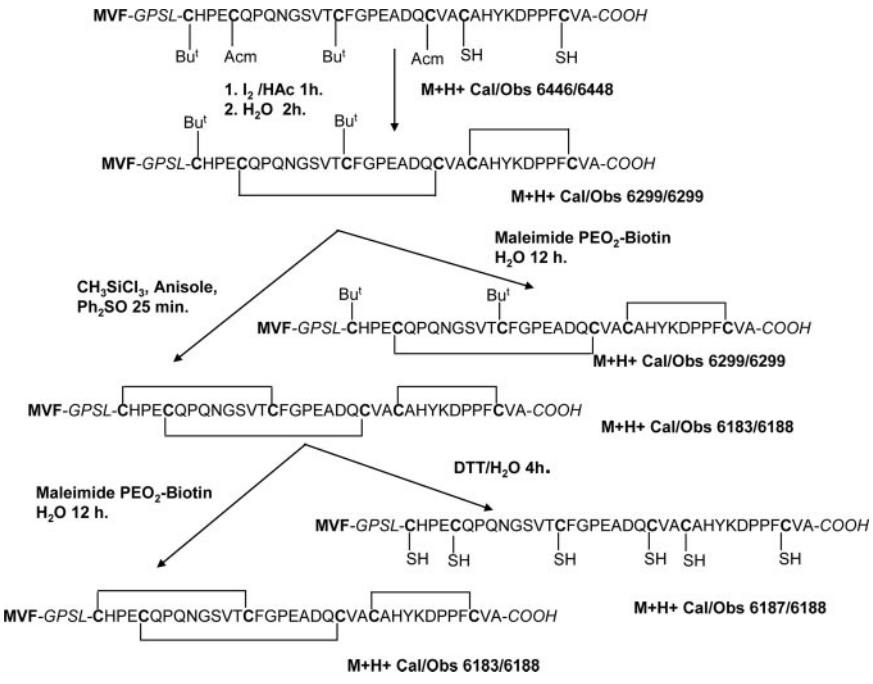


**FIGURE 1.** Synthetic strategy for generating three disulfide pairings in peptide MVF*GPSL*-563–598 from the trastuzumab-binding region of HER-2. Disulfide bonds are selectively introduced in the epitope; the peptide was synthesized with chemoselective protected cysteine residues. Each cysteine pair of a disulfide bond was identically protected to achieve desired intramolecular cyclization. The PEO-maleimide reaction and subsequent ESI-MS characterization confirmed the intramolecular disulfide pairing.

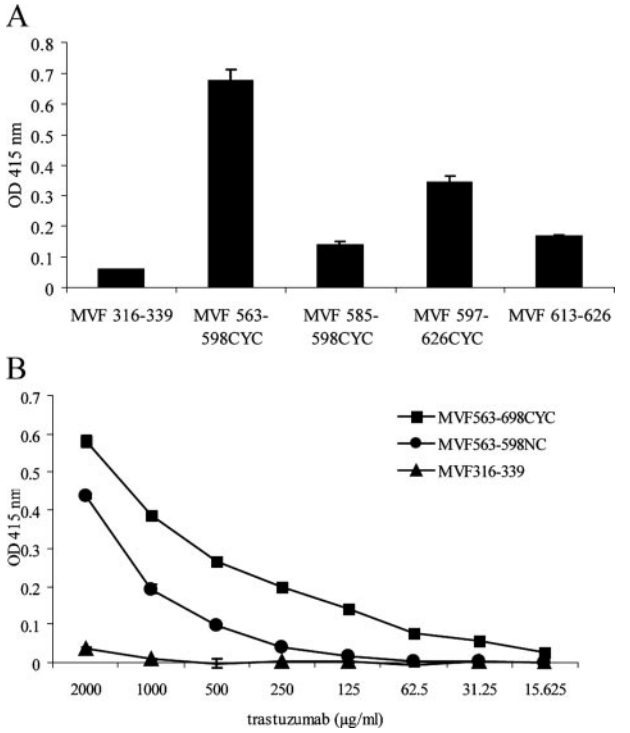


**FIGURE 2.** Binding of trastuzumab to peptides. Microtiter wells were coated overnight with 2 $\mu$g/ml various peptides and then blocked with 1% BSA for 1 h. Trastuzumab was then added to plates at a concentration of 2000 $\mu$g/ml and serially diluted 1/2 with PBT. Bound trastuzumab was detected with HRP-conjugated anti-human IgG and then with substrate. *A*, The $OD_{415}$ value for peptides from Table I and an irrelevant control peptide (MVF316–339) using 2000 $\mu$g/ml trastuzumab. Values shown are the mean of duplicate samples. SEM are indicated by error bars. *B*, Titration of trastuzumab with the disulfide-bound (CYC) and linear (NC) forms of MVF563–598 along with irrelevant control peptide (MVF316–339).

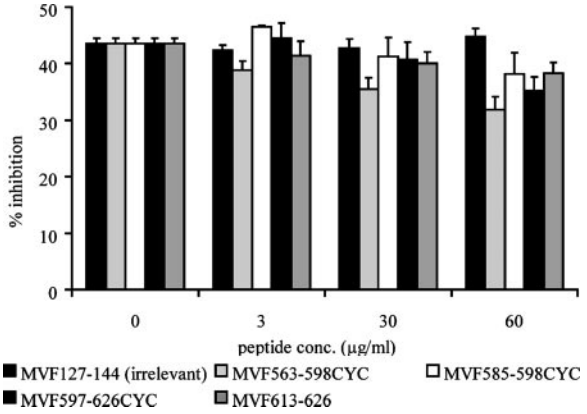


**FIGURE 3.** Cell proliferation by MTT assay. BT474 cells were plated in 96-well microtiter plates at $2 \times 10^4$ cells/well and incubated overnight at 37°C. PBS containing trastuzumab or normal human IgG (100 $\mu$g/ml) with or without peptide at the indicated concentrations was added to the wells. MVF127–144 is an irrelevant control peptide. The plates were incubated for 3 days at 37°C. The number of viable cells was measured with MTT by reading $OD_{570}$. The percentage of inhibition was calculated using the formula $(OD_{\text{normal human IgG}} - OD_{\text{trastuzumab + peptide}})/OD_{\text{normal human IgG}} \times 100$. Values shown are the mean of triplicate samples. SEM are indicated by error bars.

of control peptide had no effect (Fig. 3). At a concentration of 60 $\mu$g/ml only the 563–598 and 597–626 peptides had a statistically significant decrease ($p < 0.05$) in inhibition compared with nonspecific peptide (MVF 127–144), indicating that both MVF 563–598CYC and MVF 597–626CYC peptides bind to trastuzumab and prevent the mAb from inhibiting tumor cell growth.

*Immune response of peptide constructs in FVB/n mice*

We investigated the immune response of each of these constructs in FVB/N mice ($n$ = 5–10). Each of the constructs elicited high-titered Abs in mice, as evidenced by Ab titers over 100,000 (Fig. 4*A*). Notably both the cyclized (CYC) and linear (NC) forms of the 563–598 epitope were most immunogenic and induced titers greater than 100,000 in each mouse 2 wk after the second booster injection. In addition, mice receiving the cyclized versions of 563–598 and 597–626 showed a greater immune response compared with mice receiving the linear versions of the peptides. IgG1, IgG2a, and IgG2b were the major isotypes in the mouse sera elicited by the various peptide constructs (Fig. 4*B*). Interestingly, sera against peptide constructs MVF 585–598CYC, MVF 597–626CYC, and MVF 597–626NC generated the largest proportion of IgG2a (29–32% of total Ig), an isotype associated with an effective antitumor response (28, 32, 33).

*Cross-reactivity of the peptide Abs with native HER-2*

It is essential for Abs raised against a synthetic peptide to recognize the native protein to be considered a potential vaccine candidate. We tested the binding of FVB/N purified Abs to the HER-2-overexpressing human breast cancer lines BT474 and SK-BR-3 by immunofluorescence staining of a single-cell suspension (Fig. 5, *left* and *middle panel*). Abs generated against 597–626 bound well within 1 log of HER-2-specific mouse mAb Ab-2 in both BT474 and SK-BR-3 (Fig. 5*C*) cell lines and showed the largest shift of the anti-peptide Abs. Abs against the 613–626 epitope were capable of recognizing the native protein (Fig. 5*D*). However, Abs to 563–598 and 585–598 showed weak binding to both cell lines (Fig. 5, *A* and *B*).

Anti-peptide Abs did not demonstrate binding to MDA468 (Fig. 5, *right panel*), a non-HER-2-overexpressing breast cancer cell line. The 563–598 sequence harbors a putative *N*-linked glycosylation site at residue 571 (Table I, boxed residues). The published crystal structure of HER-2 bound to trastuzumab was enzymatically deglycosylated, whereas the crystal structure of HER-2 bound to the pertuzumab Fab reveals a sugar moiety at position 571 (34). Abs against 563–598 peptides did not cross-react with SK-BR-3 cells treated with tunicamycin, which prevents addition of *N*-linked oligosaccharides to proteins (data not shown). The lack of recognition of Abs elicited to 563–598 may be due to conformational differences when HER-2 is glycosylated. The 585–598 epitope is most likely too short (containing only 14 aa) to elicit cross-reactive Abs specific to HER-2.

*Effects of 597–626 peptide constructs in outbred rabbits*

Based on the ability of Abs induced by the synthetic peptide vaccine 597–626 to bind the native receptor with high specificity and to be recognized by trastuzumab, this epitope was considered to be the most promising vaccine candidate. We therefore evaluated the immunogenicity of the 597–626 construct in outbred New Zealand White rabbits to generate a large quantity of Abs for in vitro studies. Both the cyclized and linear peptides elicited high-titered Abs (Fig. 6*A*).

IgG was the predominant isotype generated in rabbits. Abs elicited by 597–626 CYC construct contained 95.8% IgG, 3.7% IgM, and 0.5% IgA, whereas Abs elicited against 597–626NC had 94.4% IgG, 5.0% IgM, and 0.6% IgA (data not shown). We examined the cross-reactivity of the rabbit Abs to the native protein using flow cytometry. Abs raised against both 597–626CYC and NC recognized both HER-2-overexpressing cell lines BT474 (Fig.

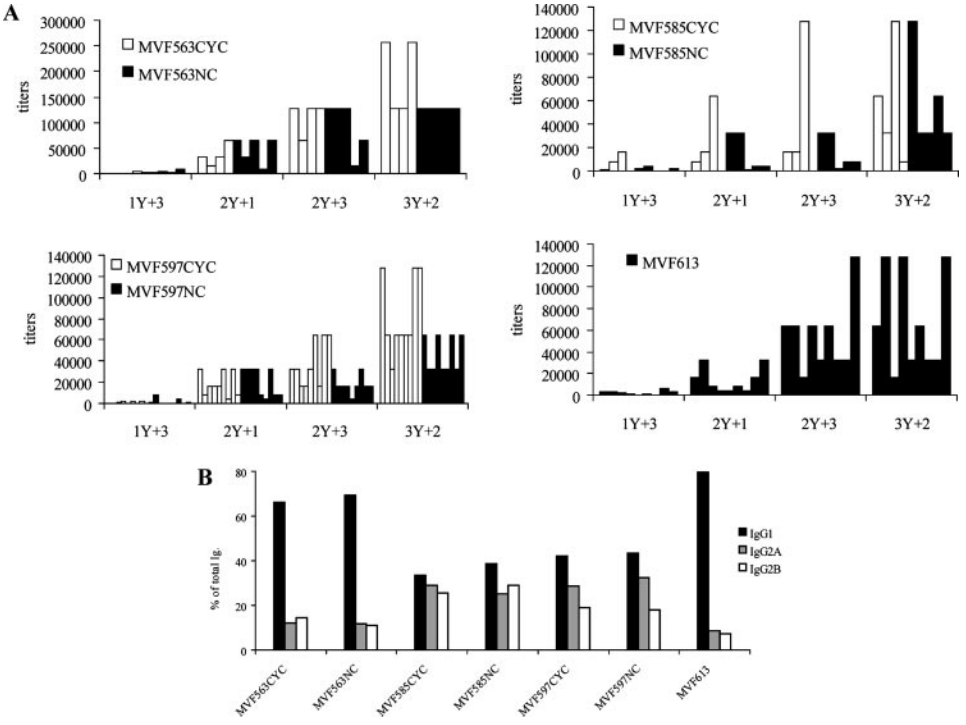


**FIGURE 4.** Immunogenicity of HER-2 peptide constructs in FVB/N mice. *A*, Indirect ELISAs were performed; results of individual mice are shown ($n$ = 5–10). Ab titers were defined as the reciprocal of the highest serum dilution with an absorbance of 0.2 or greater after subtracting the background. 1y + 3 indicates the titer of blood drawn 3 wk after the first immunization. Preimmune sera was used as a negative control (data not shown). *B*, Two weeks after the final immunization (3Y + 2), the level of Ig subtypes were measured using a mouse isotyping kit. The concentrations of IgG3, IgA, and IgM were <10% (data not shown).

6*B*) and SK-BR-3 (Fig. 6*C*) but MDA468 cells (Fig. 6*D*) which do not overexpress HER-2. This data suggest that the Abs induced by the vaccine constructs were specific for the HER-2 protein. In addition, the binding of anti-peptide Abs to HER-2 was measured using two ELISA. First, we performed a sandwich ELISA in which SK-BR-3 cell lysate was used as a source of HER-2. Fig. 7*A* reveals that anti-597–626 Abs (1/100 dilution) recognize HER-2 in a similar manner as trastuzumab (20 $\mu$g/ml). Next, the ability of 597–626 anti-peptide Abs to bind recombinant human HER-2/Fc chimera was examined. Both 597–626CYC and 597–626NC Abs had a titer of 8000 (Fig. 7*B*) against the native protein. To test whether the 597–626 anti-peptide Abs bound to the same epitope as trastuzumab, the mAb or isotype control human IgG were used as competitor for Ag binding in ELISA experiments. Anti-peptide Abs were allowed to bind to immobilized HER-2 in the presence and absence of various concentrations of trastuzumab or human IgG. At a concentration of 1000 ng/ml, trastuzumab was able to inhibit the binding of anti-597–626CYC Abs (Fig. 7*C*) and anti-597–626NC Abs (Fig. 7*D*) to HER-2 by 75.0 and 70.9%, respectively. The results demonstrate that both anti-597–626CYC and anti-597–626NC Abs recognize the same or similar determinant as that of trastuzumab.

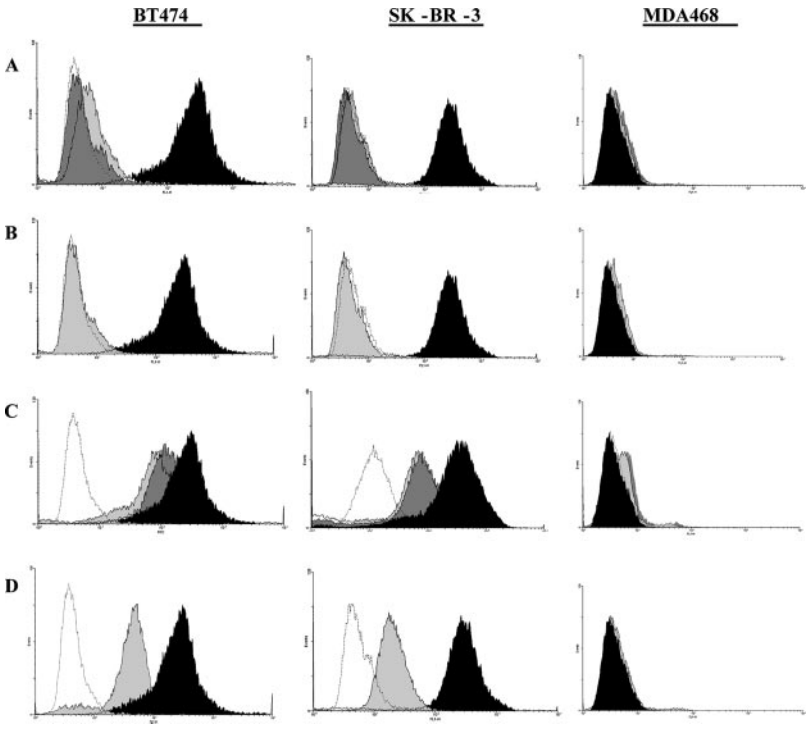


**FIGURE 5.** Cross-reactivity of peptide Abs to breast cancer cell lines. The reactivity of purified Abs from immunized FVB/n mouse sera was tested with BT474 (*left panel*), SK-BR-3 (*middle panel*), which are breast cancer cell lines that overexpress HER-2, and MDA468 (*right panel*), a non-HER-2 overexpressing cell line, using flow cytometric analysis. Abs shown were raised against peptides (*A*) 563–598, (*B*) 585–598, (*C*) 597–626, and (*D*) 613–626. Ab binding was detected with goat-anti-mouse FITC-conjugated secondary abs. Histograms indicate linear peptide Abs (light gray shading), cyclized peptide Abs (dark gray shading), normal mouse IgG (negative control, light gray line histogram), and Ab-2 (positive control, black shading).

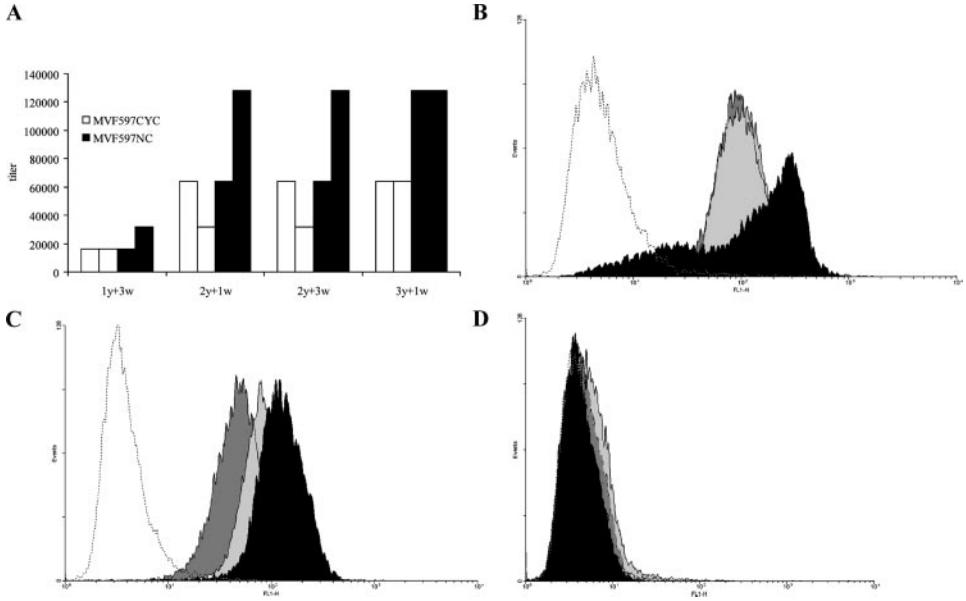


**FIGURE 6.** Effect of vaccination with 597–626 epitope in outbred rabbits. *A*, Indirect ELISAs were performed to determine the immunogenicity of the cyclized and linear constructs in pairs of outbred rabbits. Ab titers were defined as the reciprocal of the highest serum dilution with an absorbance of 0.2 or greater after subtracting the background. 1y + 3w indicates the titer of blood drawn 3 wk after the first immunization. Preimmune sera was used as a negative control (data not shown). (*B*) BT474, (*C*) SK-BR-3, and (*D*) MDA468 cells were incubated with peptide vaccine induced Abs; the extent of tumor binding was assessed by flow cytometry. Histograms indicate 597NC Abs (light gray shading), 597CYC (dark gray shading), normal rabbit IgG (negative control, dotted line histogram), and trastuzumab (positive control, black shading).

*Effect on breast cancer cell viability and proliferation*

We next examined the effect of 597–626 peptide Abs on tumor cell survival in vitro (29). BT474 cells were plated overnight; the next day cells were treated with either 20 $\mu$g/ml Abs elicited from 597CYC, 597NC, trastuzumab, normal rabbit IgG, or medium alone. Cell viability was measured after 72 h by trypan blue exclusion. Cells treated with Abs elicited from 597–626CYC and 597–626NC had 61 and 46% viability, respectively, compared with untreated cells (Fig. 8*A*) whereas trastuzumab treated cells had 21% viability, indicating that Abs against both conformational

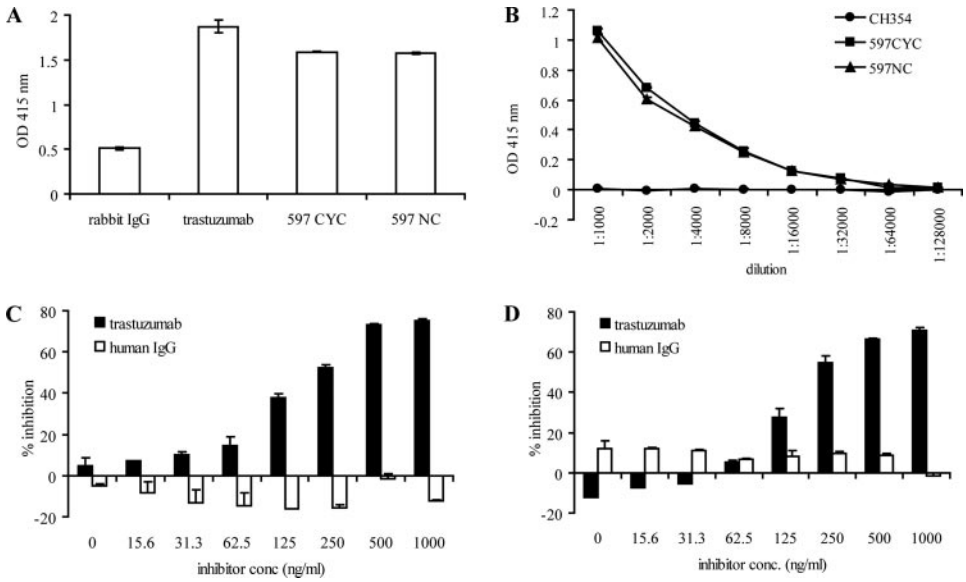


**FIGURE 7.** ELISA data demonstrating anti-597–626 Abs bind HER-2 and trastuzumab inhibits anti-597–626 Abs binding to HER-2. *A*, A sandwich ELISA was conducted to evaluate Abs specific to HER-2. SK-BR-3 cell lysate was added to plates containing capture Ab Ab-2. Sera was analyzed at 1/100 along with 20 $\mu$g/ml trastuzumab (positive control). *B–D*, Plates were coated overnight with 500 ng/ml recombinant human HER-2/Fc chimera. *B*, Serial dilution of rabbit anti-597 Abs and anti-CH354 Abs (irrelevant control) starting at a 1/1000 dilution were added to plates. The *x*-axis represents dilution of rabbit sera. *C* and *D*, A constant amount (1/2000 dilution) of rabbit anti-597–626 CYC abs (*C*) or anti-597–626 NC Abs (*D*) was added to the plates and at the same time various amounts of inhibitor (trastuzumab or isotype control human IgG) were added. Bound anti-peptide rabbit Abs were detected with HRP-conjugated anti-rabbit IgG Ab and then substrate. The *x*-axis represents concentration of inhibitor trastuzumab or human IgG. The inhibition rate was calculated according to the following formula: $(OD_{\text{anti-peptide Ab}} - OD_{\text{anti-peptide Ab + inhibitor}})/(OD_{\text{anti-peptide Ab}}) \times 100$. Values shown are the mean of duplicate samples. SEM are indicated by error bars.

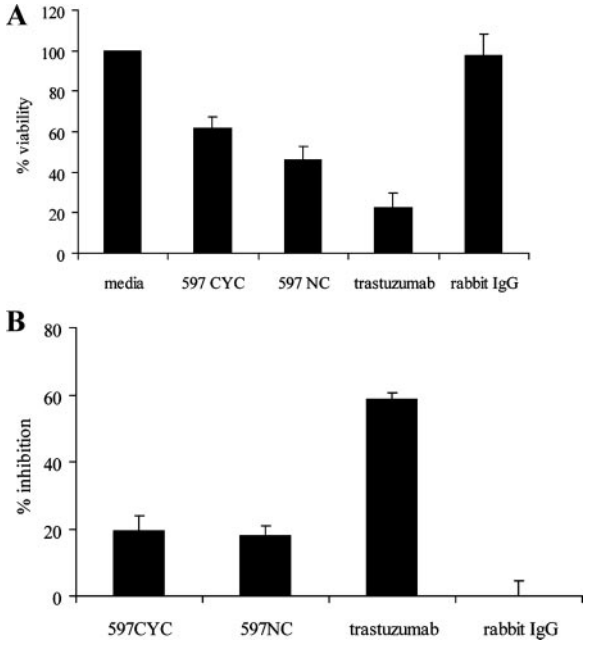


**FIGURE 8.** Anti-peptide Abs decrease cell viability and inhibit tumor cell proliferation in vitro. *A*, Trypan blue exclusion assay showing the effects of purified anti-peptide Abs on the viability of BT474 cells. A total of $1 \times 10^5$ cells were incubated with medium alone, 597CYC Abs, 597NC Abs, trastuzumab, and normal rabbit IgG (20 $\mu$g). The number of viable cells remaining after 3 days was determined by the trypan blue exclusion assay. Cell viability is given as a percentage of untreated cells. Data points represent the mean of three independent experiments; bars represent SEM. *B*, Effects of purified anti-peptide Abs on the proliferation of BT474 cells. A total of $1 \times 10^4$ cells was incubated with 597CYC Abs, 597NC Abs, trastuzumab, and normal rabbit IgG (0.1 $\mu$g). Bioconversion of MTT was used to estimate the number of viable tumor cells remaining after 3 days. The proliferation inhibition rate was calculated using the formula $(OD_{\text{normal rabbit IgG}} - OD_{\text{peptide Ab}})/OD_{\text{normal rabbit IgG}} \times 100$. Error bars represent SEM.

and linear form of 597–626 are able to decrease BT474 cell viability. We then examined the ability of anti-peptide Abs to effect in vitro tumor cell proliferation using the MTT assay. As shown in Fig. 8*B* Abs elicited by peptide epitopes 597CYC and 597NC had a similar effect on the proliferation of BT474 cells (19 and 18% inhibition, respectively), whereas trastuzumab demonstrated a 59% inhibition on tumor cell proliferation. These findings demonstrate that Abs against both conformational and linear forms of 597–626 are able to diminish cell viability as well as have antiproliferative effects on BT474 cells in vitro.

### *Ability of anti-peptide Abs to mediate ADCC*

It has been well-documented that in vivo the Fc portions of Abs can be of foremost importance for efficacy against tumor targets (35). When Fc binding is reduced or completely removed, trastuzumab loses virtually all of its antitumor activity in vivo (36). Consequently, Fc-dependent ADCC is critical for in vivo efficacy. Therefore, we measured the ability of the anti-peptide Abs to mediate ADCC in vitro. Peptide Abs elicited in rabbits against both the cyclized and linear peptide invoked lysis of the breast cancer cell line BT474 in the presence of human PBMCs, analogous to trastuzumab (Fig. 9). These results suggest that Abs raised against both conformational and linear form of 597–626 are able to mediate ADCC in a similar manner as trastuzumab.

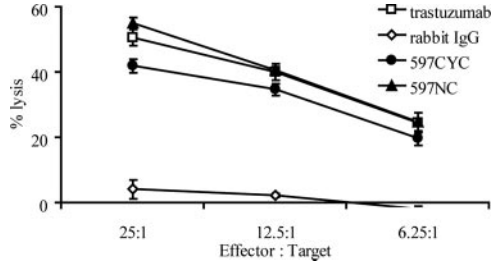


**FIGURE 9.** Anti-peptide Abs are capable of mediating ADCC. $^{51}$Cr-labeled mammary tumor target cell line BT-474 was assayed in the presence of human PBMCs. The percentage of cytotoxicity was calculated as described in *Materials and Methods*. Bars represent SEM of triplicate wells.

### *Effect of conformational restriction on the MVF 597–626 sequence*

The chimeric peptide epitopes are quite complex involving several turns, antiparallel $\beta$-sheets, $\beta$-turn, and some helical structure in the MVF epitope. Our structural analysis of the cyclized and noncyclized peptides by CD (data not shown) was quite similar involving those secondary elements. Peptide MVF 597–626CYC is partially folded because of conformational constraints imposed by one disulfide bond. This disulfide bond reduces the conformation freedom of the polypeptide chain. CD measurements (data not shown) at 100 $\mu$M concentration shows minimum at 198 nm as well as 195 nm indicating population of turns in this peptide. The peptide MVF 597–626NC shows only one minimum at 198 nm indicating different topology of

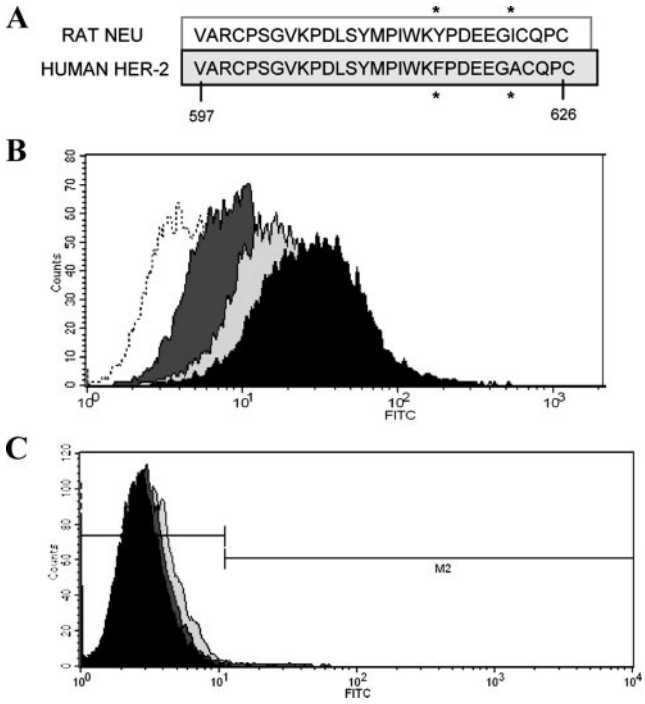


**FIGURE 10.** Cross-reactivity of HER-2 peptide Abs with the rat *neu* receptor. *A*, The amino acid sequences of rat *neu* (*top*) and human HER-2 (*bottom*, light gray shading) were aligned between human HER-2 sequence 597–626. *, Disparate residues. Flow cytometric analysis was performed on TUBO (*B*) and TS/A (*C*) cell lines. TUBO are derived from a spontaneous breast cancer of a BALB-neuT transgenic mouse and overexpress rat *neu*; TS/A is a spontaneous breast cancer from a wild-type BALB/c mouse. Histograms indicate 597NC Abs (light gray shading), 597CYC (dark gray shading), normal rabbit IgG (negative control, dotted line histogram), and Ab-4 (anti-*neu* Ab, black shading).

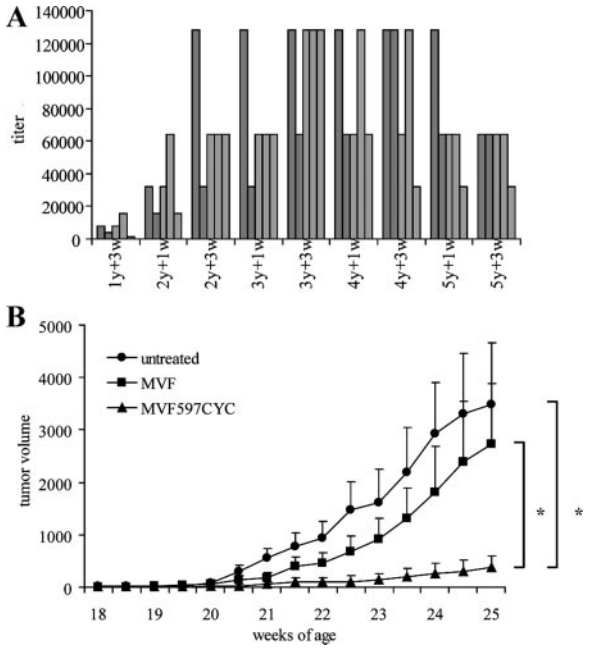


**FIGURE 11.** Immunogenicity and immunoprotective effects of HER-2 peptide epitope on autochthonous tumor development in BALB-*neu*T transgenic mice. BALB-*neu*T mice ($n = 5–7$) were immunized with MVF, MVF597CYC, or left untreated. Beginning at 5–6 wk of age, mice were treated five times at 3- to 4-wk intervals. *A*, ELISAs were performed to determine the immunogenicity of the 597CYC construct in BALB-neuT mice. Each mouse is represented by an individual box. Ab titers were defined as the reciprocal of the highest serum dilution with an absorbance of 0.2 or greater after subtracting the background. 1y + 3 indicates the titer of blood drawn 3 wk after the first immunization. *B*, Tumor measurements were performed twice a week on each of 10 mammary glands. Tumor volumes were calculated by the formula (long measurement × short measurement$^2$)/2. The data are presented as the average tumor size per group and are reported as mm$^3$. The group receiving MVF597CYC showed significant prevention of tumor growth compared with the naive group or the group receiving MVF (*, $p < 0.0001$). Error bars represent SEM.

the B cell component with lack of any constraint because of absence of disulfide bond. Both peptides do not show characteristic CD minimum of the $\beta$-sheet structure, this observation suggests the presence of isolated $\beta$-turns and constrained secondary structure in disulfide-bonded peptide construct. A plausible explanation is that this region of the protein as well as the individual peptide may fold independently and does not require constraining by disulfide bonds as they are conformationally flexible.

### *Effects of peptide constructs in BALB-neuT mice*

We used the BALB-*neu*T transgenic mouse mammary cancer model as a measure of the ability of the peptide constructs to reduce tumor progression. BALB/c inbred mice transgenic for the transforming activated rat HER-2/*neu* oncogene under the control of a mammary-specific promoter is likely the most aggressive model of HER-2/*neu* carcinogenesis (27). A point mutation that replaces the valine residue at position 664 in the transmembrane domain with glutamic acid favors HER-2/*neu* homo- and heterodimerization and renders the *neu* gene product constitutively active (37). Animals rapidly develop tumors; in preliminary studies using untreated mice, all animals developed tumors by 25 wk of age.

There is 88% sequence homology between human HER-2 and rat neu; the human 597–626 sequence has 93% homology with the rat neu sequence, with two disparate amino acids (Fig. 10*A*). We examined whether Abs raised against 597–626 were capable of recognizing the rat neu receptor using the TUBO cell line, a cell line established in vitro from a lobular carcinoma that arose spontaneously in a BALB-*neu*T mouse. As depicted in Fig. 10*B*, Abs against both cyclized and linear forms of 597–626 were shifted relative to normal rabbit IgG and were comparable to Ab-4, a mouse mAb that binds rat neu. Flow cytometric analysis of the non-neu-expressing TS/A cell line demonstrated that no Abs bound this cell line (Fig. 10*C*).

Based on these results, the conformationally restricted MVF 597–626 was chosen for study in female transgenic BALB-*neu*T mice. Previous studies have shown the age at which mice are immunized is critical (33). Transgenic mice that began receiving dendritic cells transduced with adenovirus expressing the neu oncoprotein past 6-wk old had larger tumor burden compared with mice receiving the vaccine at 5–6 wk of age (38). Transgenic mice were immunized with 597–626CYC beginning at 5–6 wk of age. Mice received two booster immunization at 3-wk intervals and subsequently two additional immunizations at 4-wk intervals. Impressively, 597CYC elicited high-titer anti-neu Ab responses in all mice 3 wk after the third immunization (Fig. 11*A*). At 25 wk of age, untreated mice and mice immunized with irrelevant peptide had an average tumor burden of 3486 mm$^3$ (±1166) and 2720 mm$^3$ (±1163), respectively ($p = 0.6441$). Mice immunized with 597–626CYC had a significant reduction in tumor burden ($p < 0.0001$), with an average tumor burden of 378 mm$^3$ (±228.0) (Fig. 11*B*). The in vivo antitumor activity observed here correlates with the in vitro studies indicating the 597–626 construct is capable of inhibiting tumor cell growth as well as mediate ADCC in a similar manner as trastuzumab. These results indicate that the conformationally restricted 597–626 epitope is capable of significantly inhibiting tumor growth in a mouse model that parallels several characteristics of the stepwise mammary carcinogenesis in women.

## Discussion

HER-2 vaccines have been designed that use whole cells expressing tumor Ags (39–41), proteins (42), as well as DNA expression plasmids (43–45). Most of the immunotherapies targeting the HER-2 oncoprotein have focused on T cell epitopes, and several studies have produced notable results indicating that vaccinated patients can develop immunity to HER-2 peptides and native protein (46–48). Recent clinical trial results using a HER-2 CTL epitope showed an increase in disease-free survival in vaccinated HER-2/neu-expressing breast cancer patients (85.7%) compared with the control group (59.8%) (49). However, the effectiveness of a CTL vaccine for clinical use is limited to patients who express the appropriate HLA haplotype. To date mAbs, based on B cell immune responses, and not vaccines to activate the T cell immune responses, have been successful in clinical trials and approved for usage (50). In particular, the clinical efficacy of trastuzumab suggests that the generation of a robust and focused humoral immune response may be biologically significant for tumor defense.

Before the publication of the three-dimensional structure of HER-2 (20), the identification of HER-2 B cell epitopes was achieved through computer-aided analysis (18, 19, 51). In addition, several HER-2 B cell mimotopes have been identified through phage display (11, 52, 53). Riemer et al. (52) used a constrained 10-mer random peptide phage display library to identify peptide mimotopes to trastuzumab; Abs raised against one of these peptides recognized HER-2/neu and caused internalization of the receptor from the cell surface in a similar manner as trastuzumab (52). Although this peptide sequence bears no sequence homology to HER-2, it was matched to the third loop of HER-2 at the HER-2/trastuzumab interface using computational methods (54). Jiang

et al. (53) identified another mimotope that matched to an epitope between loops 1 and 2 of HER-2 at the HER-2/trastuzumab interface. These studies indicate that all three loops are important for trastuzumab-binding HER-2.

We have designed four peptide constructs that each contains at least one of the three loops of HER-2 involved in binding trastuzumab. The use of synthetic peptides to represent protein domains is restricted by conformational issues. The protein fragment of interest is stabilized by secondary and tertiary interactions in the native protein, but the matching peptide in solution will typically have a random coil structure. Lacking structural restraints, the flexibility of peptides can lead to varied conformations presented to the immune system, most of which are non-native (55). Linear peptides are highly flexible and can adopt a variety of conformations in solution. However, only a few of these conformations are responsible for their immunoreactivity (56). One approach to achieve molecular mimicry to the parent protein is through constricting the peptide by cyclization if the natural sequence bears cysteine residues that are paired to provide loop sequences with enhanced stability. Cyclic peptides can cause preferred spatial arrangements that duplicate the bioactive conformation, resulting in improved binding and immunological properties.

In our previous studies, we demonstrated that conformational cyclic epitopes HER-2 sequence 626–649 (24) had the desired secondary structural characteristics as determined by CD measurements. Abs against the cyclized epitope bound the HER-2 protein with a higher affinity than the noncyclized epitope and were twice as effective in ADCC assay and in reducing tumor growth in transgenic mice. However, in the present study, we were unable to differentiate between the conformations of the epitope region spanning residues 597–626. Similarly, the Abs that were generated were also very similar in reactivity and biological efficacy.

We have designed peptide constructs to include the native disulfide bonds of the epitopes to more closely mimic the native structure. Each of the peptide constructs were recognized by trastuzumab, with 563–598 showing the greatest recognition. In addition, all peptides were able to prevent trastuzumab from inhibiting tumor cell growth. However, Abs raised against the 563–598 epitope do not, to an appreciable extent, recognize HER-2 as measured by flow cytometry.

This may be due to the asparagine-linked glycosylation site (571-NGS) found within this sequence. It has been reported previously that trastuzumab's mouse counterpart mAb, 4D5 recognized glycosylated HER-2 and unglycosylated HER-2, indicating that either the mAb recognizes a conformation of the protein attained only when it is glycosylated, or, conversely, the epitope recognized by 4D5 comprises partly of carbohydrate (57). Abs against the 563–598 peptide inability to bind native HER-2 may due to a local conformational change when HER-2 is glycosylated, or, alternatively, dominant epitopes in the 563–598 peptide are not surface exposed on the native protein. However, Abs raised against the third loop of HER-2 (597–626) did recognize HER-2 and were investigated further. The 597–626 epitope was immunogenic in outbred rabbits; these polyclonal Abs recognized HER-2. In addition, competition experiments revealed that trastuzumab was able to inhibit the binding of anti-597 Abs to HER-2, indicating the anti-peptide Abs bound the same epitope as trastuzumab.

Trastuzumab is known to affect tumor growth by both direct and indirect mechanisms. The direct mechanisms involve binding to HER-2 and altering the receptor's signaling properties that can result in tumor growth cell inhibition (13). Anti-597 Abs were able to diminish cell viability as well as inhibit tumor cell growth of the BT474 cell line in a similar manner as trastuzumab. The indirect mechanisms involve the classical pathways in which trastuzumab kills tumor cells by mediating ADCC and CDC. We show here that anti-597 Abs were able to mediate ADCC in a manner similar to trastuzumab. Although the mechanisms by which Abs exert their therapeutic effects are still being debated, the putative mechanisms are either direct (i.e., block signaling functions, internalization of receptors, reduce proteolytic cleavage of receptors) or indirect action mediated by the immune system CDC, ADCC. Thus, we have attributed the antitumor response and protective efficacy to the generation of anti-peptide Abs and not to a T cell-mediated immune response. However, because we did not evaluate the types of tumor infiltrating leukocytes that may have been induced after peptide vaccination or in mammary tumors of BALB-*neu*T mice after defined stages, we cannot discount the possibility that a T cell response ($CD8^+$ or $CD4^+$) to the vaccine may have played a role in efficacy. In future studies, we will explore the tumor microenvironment and its interface with the tumor cells because it is known that some tumors are infiltrated with lymphocytes, macrophages, and granulocytes.

To demonstrate in vivo efficacy of the 597–626 vaccine, we used the BALB-*neu*T transgenic mouse model. Although a more desirable model would be mice transgenic for human HER-2, only recently has a model been described in which animals form tumors (58). Abs against the 597–626 epitope were cross-reactive with rat neu protein, thus we used this animal model. It has been shown that the induction of anti-HER-2/neu Abs are both necessary and sufficient for protection of BALB-*neu*T mice from developing tumors as shown by depletion of $CD4^+$ and $CD8^+$ cells (32, 33). Thus, this animal model is advantageous to studies that identify B cell epitopes necessary in the protection of BALB-*neu*T transgenic mice from developing tumors. By 25 wk of age, mice immunized with the 597CYC construct had a statistically significant reduction in tumor burden compared with both naive and MVF-immunized mice. Because we have demonstrated that Abs against the 597–626 epitope bind to HER-2 at the trastuzumab interface, the mechanism of action of the endogenous tumor protective in BALB-*neu*T mice most likely include down modulation of the HER-2/*neu* receptor as well as interaction with the immune system via the Fc domain of endogenous Abs against the 597–626 epitope.

In summary, we report here an epitope that mimic the HER-2/trastuzumab interface capable of inducing Abs with antitumor properties that significantly reduces tumor burden in vivo in transgenic mice. There are inherent limitations of passive immunotherapy with trastuzumab including unequal tissue distribution, limited half-life, prolonged administration, possible immunogenicity with high dosages, and cardiotoxicity. Immunotherapy with peptide vaccines that produces endogenous Abs may be more valuable than repeated administration of an exogenous mAb. Peptide vaccines are easy to produce, amenable to quality control, and cost effective. The active generation of Abs with similar characteristics as trastuzumab has the potential to suppress the development of HER-2-overexpressing breast cancers.

## Disclosures

The authors have no financial conflict of interest.

## References

1. Coussens, L., T. L. Yang-Feng, Y. C. Liao, E. Chen, A. Gray, J. McGrath, P. H. Seeburg, T. A. Libermann, J. Schlessinger, U. Francke, et al. 1985. Tyrosine kinase receptor with extensive homology to EGF receptor shares chromosomal location with *neu* oncogene. *Science* 230: 1132–1139.
2. Karunagaran, D., E. Tzahar, R. R. Beerli, X. Chen, D. Graus-Porta, B. J. Ratzkin, R. Seger, N. E. Hynes, and Y. Yarden. 1996. ErbB-2 is a common auxiliary

subunit of NDF and EGF receptors: implications for breast cancer. *EMBO J.* 15: 254–264.
3. Klapper, L. N., S. Glathe, N. Vaisman, N. E. Hynes, G. C. Andrews, M. Sela, and Y. Yarden. 1999. The ErbB-2/HER2 oncoprotein of human carcinomas may function solely as a shared coreceptor for multiple stroma-derived growth factors. *Proc. Natl. Acad. Sci. USA* 96: 4995–5000.
4. Press, M. F., C. Cordon-Cardo, and D. J. Slamon. 1990. Expression of the HER-2/*neu* proto-oncogene in normal human adult and fetal tissues. *Oncogene* 5: 953–962.
5. Slamon, D. J., W. Godolphin, L. A. Jones, J. A. Holt, S. G. Wong, D. E. Keith, W. J. Levin, S. G. Stuart, J. Udove, A. Ullrich, and M. F. Press. 1989. Studies of the HER-2/*neu* proto-oncogene in human breast and ovarian cancer. *Science* 244: 707–712.
6. Cirisano, F. D., and B. Y. Karlan. 1996. The role of the HER-2/*neu* oncogene in gynecologic cancers. *J. Soc. Gynecol. Investig.* 3: 99–105.
7. Berchuck, A., G. Rodriguez, R. B. Kinney, J. T. Soper, R. K. Dodge, D. L. Clarke-Pearson, and R. C. Bast, Jr. 1991. Overexpression of HER-2/*neu* in endometrial cancer is associated with advanced stage disease. *Am. J. Obstet. Gynecol.* 164: 15–21.
8. Kern, J. A., D. A. Schwartz, J. E. Nordberg, D. B. Weiner, M. I. Greene, L. Torney, and R. A. Robinson. 1990. p185*neu* expression in human lung adenocarcinomas predicts shortened survival. *Cancer Res.* 50: 5184–5187.
9. Ward, R. L., N. J. Hawkins, D. Coomber, and M. L. Disis. 1999. Antibody immunity to the HER-2/*neu* oncogenic protein in patients with colorectal cancer. *Hum. Immunol.* 60: 510–515.
10. Slamon, D. J., G. M. Clark, S. G. Wong, W. J. Levin, A. Ullrich, and W. L. McGuire. 1987. Human breast cancer: correlation of relapse and survival with amplification of the HER-2/*neu* oncogene. *Science* 235: 177–182.
11. Yip, Y. L., G. Smith, J. Koch, S. Dubel, and R. L. Ward. 2001. Identification of epitope regions recognized by tumor inhibitory and stimulatory anti-ErbB-2 monoclonal antibodies: implications for vaccine design. *J. Immunol.* 166: 5271–5278.
12. Sliwkowski, M. X., J. A. Lofgren, G. D. Lewis, T. E. Hotaling, B. M. Fendly, and J. A. Fox. 1999. Nonclinical studies addressing the mechanism of action of trastuzumab (Herceptin). *Semin. Oncol.* 26: 60–70.
13. Yip, Y. L., and R. L. Ward. 2002. Anti-ErbB-2 monoclonal antibodies and ErbB-2-directed vaccines. *Cancer Immunol. Immunother.* 50: 569–587.
14. Romond, E. H., E. A. Perez, J. Bryant, V. J. Suman, C. E. Geyer, Jr., N. E. Davidson, E. Tan-Chiu, S. Martino, S. Paik, P. A. Kaufman, et al. 2005. Trastuzumab plus adjuvant chemotherapy for operable HER2-positive breast cancer. *N. Engl. J. Med.* 353: 1673–1684.
15. Piccart-Gebhart, M. J., M. Procter, B. Leyland-Jones, A. Goldhirsch, M. Untch, I. Smith, L. Gianni, J. Baselga, R. Bell, C. Jackisch, et al. 2005. Trastuzumab after adjuvant chemotherapy in HER2-positive breast cancer. *N. Engl. J. Med.* 353: 1659–1672.
16. Schneider, J. W., A. Y. Chang, and A. Garratt. 2002. Trastuzumab cardiotoxicity: speculations regarding pathophysiology and targets for further study. *Semin. Oncol.* 29: 22–28.
17. Keefe, D. L. 2002. Trastuzumab-associated cardiotoxicity. *Cancer* 95: 1592–1600.
18. Dakappagari, N. K., D. B. Douglas, P. L. Triozzi, V. C. Stevens, and P. T. Kaumaya. 2000. Prevention of mammary tumors with a chimeric HER-2 B-cell epitope peptide vaccine. *Cancer Res.* 60: 3782–3789.
19. Dakappagari, N. K., J. Pyles, R. Parihar, W. E. Carson, D. C. Young, and P. T. Kaumaya. 2003. A chimeric multi-human epidermal growth factor receptor-2 B cell epitope peptide vaccine mediates superior antitumor responses. *J. Immunol.* 170: 4242–4253.
20. Cho, H. S., K. Mason, K. X. Ramyar, A. M. Stanley, S. B. Gabelli, D. W. Denney, Jr., and D. J. Leahy. 2003. Structure of the extracellular region of HER2 alone and in complex with the herceptin Fab. *Nature* 421: 756–760.
21. Kaumaya, P. T., A. M. VanBuskirk, E. Goldberg, and S. K. Pierce. 1992. Design and immunological properties of topographic immunogenic determinants of a protein antigen (LDH-C4) as vaccines. *J. Biol. Chem.* 267: 6338–6346.
22. Kobs-Conrad, S., H. Lee, A. M. DiGeorge, and P. T. Kaumaya. 1993. Engineered topographic determinants with $\alpha\beta$, $\beta\alpha\beta$, and $\beta\alpha\beta\alpha$ topologies show high affinity binding to native protein antigen (lactate dehydrogenase-C4). *J. Biol. Chem.* 268: 25285–25295.
23. Sundaram, R., M. P. Lynch, S. V. Rawale, Y. Sun, M. Kazanji, and P. T. Kaumaya. 2004. De novo design of peptide immunogens that mimic the coiled coil region of human T-cell leukemia virus type-1 glycoprotein 21 transmembrane subunit for induction of native protein reactive neutralizing antibodies. *J. Biol. Chem.* 279: 24141–24151.
24. Dakappagari, N. K., K. D. Lute, S. Rawale, J. T. Steele, S. D. Allen, G. Phillips, R. T. Reilly, and P. T. Kaumaya. 2005. Conformational HER-2/*neu* B-cell epitope peptide vaccine designed to incorporate two native disulfide bonds enhances tumor cell binding and antitumor activities. *J. Biol. Chem.* 280: 54–63.
25. Chen, Y. H., J. T. Yang, and K. H. Chau. 1974. Determination of the helix and $\beta$ form of proteins in aqueous solution by circular dichroism. *Biochemistry* 13: 3350–3359.
26. Greenfield, N., and G. D. Fasman. 1969. Computed circular dichroism spectra for the evaluation of protein conformation. *Biochemistry* 8: 4108–4116.
27. Boggio, K., G. Nicoletti, E. Di Carlo, F. Cavallo, L. Landuzzi, C. Melani, M. Giovarelli, I. Rossi, P. Nanni, C. De Giovanni, et al. 1998. Interleukin 12-mediated prevention of spontaneous mammary adenocarcinomas in two lines of Her-2/*neu* transgenic mice. *J. Exp. Med.* 188: 589–596.
28. Rovero, S., A. Amici, E. D. Carlo, R. Bei, P. Nanni, E. Quaglino, P. Porcedda, K. Boggio, A. Smorlesi, P. L. Lollini, et al. 2000. DNA vaccination against rat her-2/Neu p185 more effectively inhibits carcinogenesis than transplantable carcinomas in transgenic BALB/c mice. *J. Immunol.* 165: 5133–5142.
29. Nahta, R., L. X. Yuan, B. Zhang, R. Kobayashi, and F. J. Esteva. 2005. Insulin-like growth factor-I receptor/human epidermal growth factor receptor 2 heterodimerization contributes to trastuzumab resistance of breast cancer cells. *Cancer Res.* 65: 11118–11128.
30. Kaumaya, P. T. P., S. Kobs-Conrad, A. M. DiGeorge, and V. Stevens. 1994. Denovo engineering of protein immunogenic and antigenic determinants. In *Peptides*, Vol. 9. C. G. M. B. Anantharamaiah, ed. Birkhäuser, Boston, pp. 133–164.
31. Lairmore, M. D., A. M. DiGeorge, S. F. Conrad, A. V. Trevino, R. B. Lal, and P. T. Kaumaya. 1995. Human T-lymphotropic virus type 1 peptides in chimeric and multivalent constructs with promiscuous T-cell epitopes enhance immunogenicity and overcome genetic restriction. *J. Virol* 69: 6077–6089.
32. Nanni, P., L. Landuzzi, G. Nicoletti, C. De Giovanni, I. Rossi, S. Croci, A. Astolfi, M. Iezzi, E. Di Carlo, P. Musiani, et al. 2004. Immunoprevention of mammary carcinoma in HER-2/*neu* transgenic mice is IFN-$\gamma$ and B cell dependent. *J. Immunol.* 173: 2288–2296.
33. Park, J. M., M. Terabe, Y. Sakai, J. Munasinghe, G. Forni, J. C. Morris, and J. A. Berzofsky. 2005. Early role of $CD4^+$ Th1 cells and antibodies in HER-2 adenovirus vaccine protection against autochthonous mammary carcinomas. *J. Immunol.* 174: 4228–4236.
34. Franklin, M. C., K. D. Carey, F. F. Vajdos, D. J. Leahy, A. M. de Vos, and M. X. Sliwkowski. 2004. Insights into ErbB signaling from the structure of the ErbB2-pertuzumab complex. *Cancer Cell* 5: 317–328.
35. Clynes, R. A., T. L. Towers, L. G. Presta, and J. V. Ravetch. 2000. Inhibitory Fc receptors modulate in vivo cytoxicity against tumor targets. *Nat. Med.* 6: 443–446.
36. Clynes, R., and J. V. Ravetch. 1995. Cytotoxic antibodies trigger inflammation through Fc receptors. *Immunity* 3: 21–26.
37. Gullick, W. J., A. C. Bottomley, F. J. Lofts, D. G. Doak, D. Mulvey, R. Newman, M. J. Crumpton, M. J. Sternberg, and I. D. Campbell. 1992. Three dimensional structure of the transmembrane region of the proto-oncogenic and oncogenic forms of the neu protein. *EMBO J.* 11: 43–48.
38. Sakai, Y., B. J. Morrison, J. D. Burke, J. M. Park, M. Terabe, J. E. Janik, G. Forni, J. A. Berzofsky, and J. C. Morris. 2004. Vaccination by genetically modified dendritic cells expressing a truncated *neu* oncogene prevents development of breast cancer in transgenic mice. *Cancer Res.* 64: 8022–8028.
39. Reilly, R. T., M. B. Gottlieb, A. M. Ercolini, J. P. Machiels, C. E. Kane, F. I. Okoye, W. J. Muller, K. H. Dixon, and E. M. Jaffee. 2000. HER-2/*neu* is a tumor rejection target in tolerized HER-2/*neu* transgenic mice. *Cancer Res.* 60: 3569–3576.
40. Nanni, P., G. Nicoletti, C. De Giovanni, L. Landuzzi, E. Di Carlo, F. Cavallo, S. M. Pupa, I. Rossi, M. P. Colombo, C. Ricci, et al. 2001. Combined allogeneic tumor cell vaccination and systemic interleukin 12 prevents mammary carcinogenesis in HER-2/*neu* transgenic mice. *J. Exp. Med.* 194: 1195–1205.
41. Cefai, D., B. W. Morrison, A. Sckell, L. Favre, M. Balli, M. Leunig, and C. D. Gimmi. 1999. Targeting HER-2/*neu* for active-specific immunotherapy in a mouse model of spontaneous breast cancer. *Int. J. Cancer* 83: 393–400.
42. Dela Cruz, J. S., S. Y. Lau, E. M. Ramirez, C. De Giovanni, G. Forni, S. L. Morrison, and M. L. Penichet. 2003. Protein vaccination with the HER2/*neu* extracellular domain plus anti-HER2/*neu* antibody-cytokine fusion proteins induces a protective anti-HER2/*neu* immune response in mice. *Vaccine* 21: 1317–1326.
43. Amici, A., F. M. Venanzi, and A. Concetti. 1998. Genetic immunization against *neu*/erbB2 transgenic breast cancer. *Cancer Immunol. Immunother.* 47: 183–190.
44. Piechocki, M. P., S. A. Pilon, and W. Z. Wei. 2001. Complementary antitumor immunity induced by plasmid DNA encoding secreted and cytoplasmic human ErbB-2. *J. Immunol.* 167: 3367–3374.
45. Pupa, S. M., A. M. Invernizzi, S. Forti, E. Di Carlo, P. Musiani, P. Nanni, P. L. Lollini, R. Meazza, S. Ferrini, and S. Menard. 2001. Prevention of spontaneous neu-expressing mammary tumor development in mice transgenic for rat proto-*neu* by DNA vaccination. *Gene Ther.* 8: 75–79.
46. Disis, M. L., J. R. Gralow, H. Bernhard, S. L. Hand, W. D. Rubin, and M. A. Cheever. 1996. Peptide-based, but not whole protein, vaccines elicit immunity to HER-2/*neu*, oncogenic self-protein. *J. Immunol.* 156: 3151–3158.
47. Disis, M. L., K. H. Grabstein, P. R. Sleath, and M. A. Cheever. 1999. Generation of immunity to the HER-2/*neu* oncogenic protein in patients with breast and ovarian cancer using a peptide-based vaccine. *Clin. Cancer Res.* 5: 1289–1297.
48. Disis, M. L., T. A. Gooley, K. Rinn, D. Davis, M. Piepkorn, M. A. Cheever, K. L. Knutson, and K. Schiffman. 2002. Generation of T-cell immunity to the HER-2/*neu* protein after active immunization with HER-2/*neu* peptide-based vaccines. *J Clin. Oncol.* 20: 2624–2632.
49. Peoples, G. E., J. M. Gurney, M. T. Hueman, M. M. Woll, G. B. Ryan, C. E. Storrer, C. Fisher, C. D. Shriver, C. G. Ioannides, and S. Ponniah. 2005.

Clinical trial results of a HER2/*neu* (E75) vaccine to prevent recurrence in high-risk breast cancer patients. *J. Clin. Oncol.* 23: 7536–7545.

50. Lollini, P. L., F. Cavallo, P. Nanni, and G. Forni. 2006. Vaccines for tumour prevention. *Nat. Rev. Cancer* 6: 204–216.
51. Jasinska, J., S. Wagner, C. Radauer, R. Sedivy, T. Brodowicz, C. Wiltschke, H. Breiteneder, H. Pehamberger, O. Scheiner, U. Wiedermann, and C. C. Zielinski. 2003. Inhibition of tumor cell growth by antibodies induced after vaccination with peptides derived from the extracellular domain of Her-2/*neu*. *Int. J. Cancer* 107: 976–983.
52. Riemer, A. B., M. Klinger, S. Wagner, A. Bernhaus, L. Mazzucchelli, H. Pehamberger, O. Scheiner, C. C. Zielinski, and E. Jensen-Jarolim. 2004. Generation of peptide mimics of the epitope recognized by trastuzumab on the oncogenic protein Her-2/*neu*. *J. Immunol.* 173: 394–401.
53. Jiang, B., W. Liu, H. Qu, L. Meng, S. Song, T. Ouyang, and C. Shou. 2005. A novel peptide isolated from a phage display peptide library with trastuzumab can mimic antigen epitope of HER-2. *J. Biol. Chem.* 280: 4656–4662.
54. Riemer, A. B., G. Kraml, O. Scheiner, C. C. Zielinski, and E. Jensen-Jarolim. 2005. Matching of trastuzumab (Herceptin) epitope mimics onto the surface of Her-2/*neu*–a new method of epitope definition. *Mol. Immunol.* 42: 1121–1124.
55. Lu, S. M., and R. S. Hodges. 2002. A de novo designed template for generating conformation-specific antibodies that recognize $\alpha$-helices in proteins. *J. Biol. Chem.* 277: 23515–23524.
56. Haro, I., and M. J. Gomara. 2004. Design of synthetic peptidic constructs for the vaccine development against viral infections. *Curr. Protein Pept. Sci.* 5: 425–433.
57. Hudziak, R. M., G. D. Lewis, M. Winget, B. M. Fendly, H. M. Shepard, and A. Ullrich. 1989. p185HER2 monoclonal antibody has antiproliferative effects in vitro and sensitizes human breast tumor cells to tumor necrosis factor. *Mol. Cell. Biol.* 9: 1165–1172.
58. Finkle, D., Z. R. Quan, V. Asghari, J. Kloss, N. Ghaboosi, E. Mai, W. L. Wong, P. Hollingshead, R. Schwall, H. Koeppen, and S. Erickson. 2004. HER2-targeted therapy reduces incidence and progression of midlife mammary tumors in female murine mammary tumor virus huHER2-transgenic mice. *Clin. Cancer Res.* 10: 2499–2511.